



Original Article

Structural, Electronic and Mechanical Properties of Few-layer Porous Nanosheet from Spheroidal Cage-like ZnO Polymorph

Le Thi Hong Lien^{1,*}, Nguyen Thi Thao², Vu Ngoc Tuoc^{1,*}

¹*School of Engineering Physics, Hanoi University of Science and Technology,
1 Dai Co Viet Road, Hai Ba Trung, Hanoi, Vietnam*

²*Hong Duc University, 565 Quang Trung, Dong Xe, Thanh Hoa, Vietnam*

Received 28 April 2020

Revised 19 May 2020; Accepted 15 July 2020

Abstract: The low-dimensional II-VI group semiconductors have recently emerged as interesting candidate materials for the tailoring of two dimensional (2D) layered structures. Herein, a series of the cage-like nanoporous composed of spheroidal hollow cages (ZnO)₁₂, cutting from the high symmetrical cubic SOD cage-like polymorph as building block, is proposed. We have performed the density-functional tight binding (DFTB+) calculations on the structural, electronic and mechanical properties of this few-layer SOD-cage-block nanosheet series, to investigate the effects of structural modification and sheet thickness on their structural, electronic, and mechanical properties. Optimized geometries, formation energy, phonon spectra, electronic band structure, and elastic tensor calculation has ensured the energetically, dynamical and mechanical stability for the sheets. Furthermore, the theoretically found nanosheet series possess an intrinsic wide direct band gap preserving from wurtzite tetragonal-based bonding. This high symmetry wide bandgap semiconductor nanosheet series and their derivatives are expected to have broad applications in photocatalysis, and biomedicine.

Keywords: Nanosheet, Porous, Density Functional Theory, Tight Binding, ZnO.

1. Introduction

To date suggesting novel 2D materials with unique electronic and optical properties of low-dimensional systems are in the focus to create the nanosheet (NS) materials, that are promising for sustainability applications, e.g. such as catalysis, biocompatible polymeric and biomedicine. Zinc oxide

*Corresponding authors.

Email address: tuoc.vungoc@hust.edu.vn

<https://doi.org/10.25073/2588-1124/vnumap.4517>

(ZnO) material, along with wurtzite and zinblende stable phases, has been found in a large number of polymorph with substantially different properties, and hence, applications. ZnO with all its phases, is one of the most important metal oxide materials in bio-medicine application due to its excellent biocompatibility, strong ultraviolet (UV) absorption and antibacterial properties. Further, ZnO nanoparticle, nanoporous crystalline and NS are promising materials for various application in optoelectronic as well as antibacterial, drug delivery and bio-imaging [1, 2].

Experimentally benefited from the most advances in self-assembly technology, various nano- and micro-scale clusters can now be organized into a variety of the ordered three-dimensional (3D) lattices, that opens up the realized possibility of designing low-dimensional nanoporous material structures from a set of atomic-level secondary building blocks [3-5]. So far, realizing ZnO in new low-density low-dimensional structures is of considerable interest. Nanoclusters, in particular cage-like spheroid, are of special interest since they offer a novel *bottom-up* mean of creating a large variety of structurally different materials without changing its common material composition such as metal oxides material compounds. Thus, beside the traditional experimental approach, many low-density structures/allotropes of ZnO have been predicted computationally from first principles theoretical calculation recently [6-11].

Since the initial work of Ref. [12, 13], Bromley et.al. have firstly proposed a "bottom up" scheme by taking stable smallest "magic cluster" nanocages, i.e. Sodalite (SOD) $(\text{ZnO})_{12}$ as secondary building blocks, proving that there is no barrier to stop their coalescing to form various possible nanocage-like porous phases such as, e.g. SOD, LTA, and FAU. On the basis of this approach we have found a novel nanoporous solid phases of $(\text{ZnO})_{16}$ -cluster-assembled novel named as AST [14], which is later confirmed by extensive structural searches using the minima hopping method of ZnO cage-like bulk phases motifs [15]. Furthermore, the extended seek for the families of possible cage-like structures of individual clusters toward the nanostructured materials design has continue with several other high symmetric "magic cluster", e.g. spheroidal cages $(\text{ZnO})_{24}$, proposing two novel cage-like nanoporous polymorphs in cubic lattice frameworks [16].

In the present work, we propose a scheme for designing a series of the cage-like porous nanosheet originated from SOD's ZnO structures. Our approach relies on the construction by the bottom up approach from the spheroid magic cluster of $(\text{ZnO})_{12}$ keeping its chemical composition unchanged. We argue that this approach could provide a viable way to design nanoporous NS models computationally. We discuss the stability and the electronic structures of these materials based on calculations within the formalism of density functional based tight binding (DFTB+) by means of the binding energy computed within DFTB+ approach, phonon calculation and lattice distortion's elastic calculation. We show that all the reported structures are wide direct band gap semiconductors. Their electronic band structures are finally examined in detail.

2. Computational Details

2.1. Theoretical structure prediction approach

In this section, following our recent approach for theoretically predicting ZnO crystal hollow structures [14,16-18], the secondary building blocks were chosen to be high in symmetries and large in HOMO-LUMO gap, which is generally believed as if criteria of stability [19,20]. Starting out from a three dimensional porous crystalline of SOD's ZnO phase, we engrave out it with layered patterns, leaving out the porous *polymeric frame work* NS of originated SOD cage-like spheroid cluster. The structure is subsequently be set layer-by-layer, added thick vacuum layers, imitating 2D model structure, symmetrized and centered to get the NS's unit cell (UC) (see Figure 1). Then structures are energetically relaxed to get the final structure reported in characteristic Table 1.

Our porous NS structures reported herein are characterized by number of mono-block layer n , denoted as SOD- n , which consist of the whole SOD cage as the secondary building blocks (see Figure 1). The odd-numbered porous NS have higher UC's symmetry than the even ones. For the illustration purpose, only the several smallest NS's structures are shown in Figure 1.

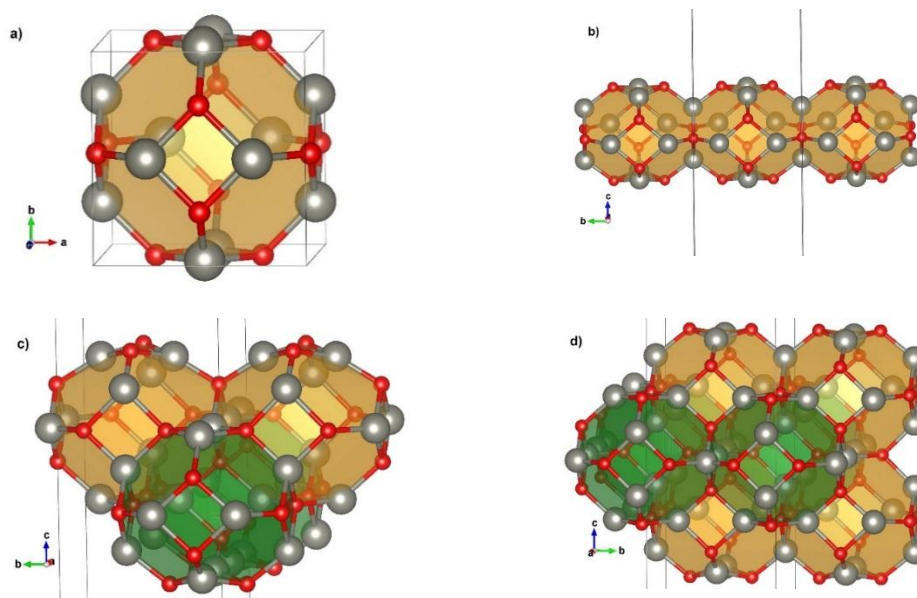


Figure 1. The ZnO porous NS structures designed in this work (a) SOD 3D bulk phase (b) SOD-1 (the NS with a monolayer of SOD cage) (c) SOD-2, (d) SOD-3. Small (red) balls are O atoms, big (gray) ones are Zn. The thin reactagular frame is the NS'd unit cell. The transparent polyhedral (orange and/or green) is to show the SOD cage-host as secondary building block.

2.2 Density functional based tight binding plus method

Our calculations were performed within the spin-polarized, charge self-consistent, density functional based tight binding plus (DFTB+) approach [21-24]. This DFTB+ method is based on a second-order expansion of the spin-dependent Kohn-Sham total energy functional with respect to a given reference charge and magnetization density. With all matrix elements and orbitals are derived from the first principles calculation, this method is benefited from on a small basis set of atomic orbitals and two-center non-orthogonal Hamiltonian, allowing extensive use of look-up table. The Kohn-Sham equations are solved self-consistently using Mulliken charge projection. The approach has been proven to give transferable and accurate interaction potential as well as numerical efficiency allowing molecular dynamic simulation of supercell containing several hundred up to a thousand atoms. In our calculations the Slater–Koster parameter set and its transferability have been successfully applied in several previous DFTB+ works [14, 25-26]. The benchmark for the DFTB+ numerical scheme used herein has been carried out in our recent study [16-18] using first principle DFT method as implemented in Vienna Ab-initio simulation package [27-28] for some ZnO hexagonal hollow structures with the Perdew-Burke-Ernzerhof (PBE) [29], PBEsol [30], and Heyd-Scuseria-Ernzerhof (HSE06) [31] functional. There comparison shows an excellent agreement between DFT and DFTB+ results and claims that DFTB+ is a reasonable method for our work.

3. Results and Discussions

3.1. Formation energy and energetic stability

During the energy relaxation process, all the designed porous NS's structures survive without structural collapse, indicating that they are physically relevant and might actually lead to low-dimensional porous NS phases of ZnO. As shown in Figure 1 as well as in the detail Characteristic Table 1, the surface reconstruction has occurred with those outer surface atom due to the dangling bonds. This causes some deformations of bond lengths and angles (see Table 1), causing the Zn atom go more inside to the NS. The influence of such surface reconstruction and the quantum confinement effect is also reflected in the band gap value. For the energetic stability, the formation energy of proposed few-layer NS with respect to their stable bulk form, which is determined by the the difference between the average energy of the NS's atoms and that of the atoms in the bulk, i.e. 3D, SOD's state. It is determined in term of *per-atom* energy by means of

$$E_{Form} = \frac{E_{NS}}{N_{atom}} - \frac{E_{SOD}^{bulk-phase}}{N_{atom}^{bulk-phase}}$$

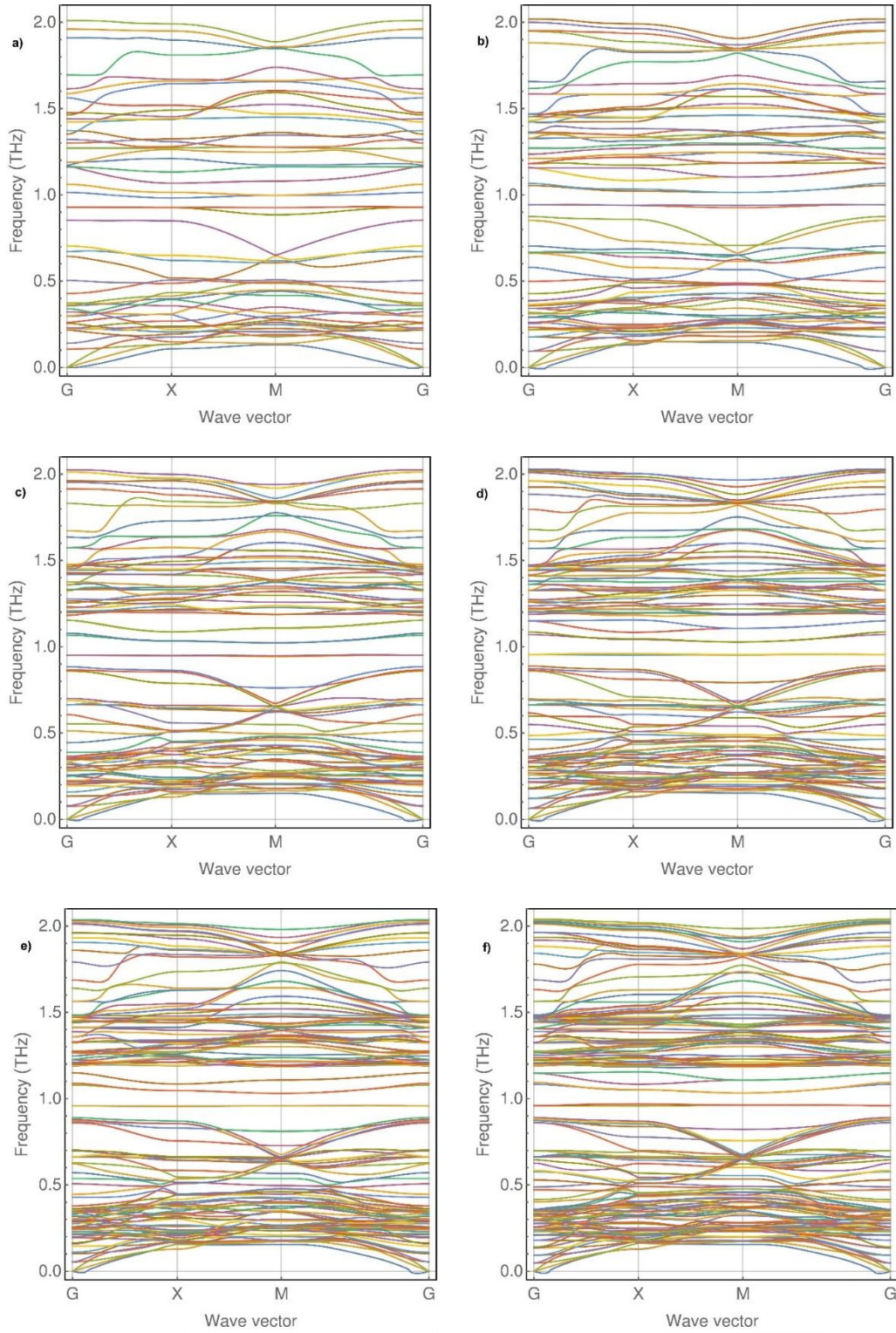
where E_{NS} is the total DFT energy of the studied NS, N_{atom} - the number of the atom in a unit cell of NS, $E_{SOD}^{bulk-phase}$ the total DFT energy the parent 3D SOD phase and $N_{atom}^{bulk-phase}$ - the number of Zn and O atoms in the SOD bulk phase unit cell. The value of formation energy w.r.t bulk porous phase in a range of 0.08-0.3 eV/atom show that the NS is in the semiconductor state as their parent bulk phase. The value of the formation energy is directly connected to the degree of the bond's distortion occurs to perfect sp^3 configuration of SOD due to dangling bond at the surface. Figure 4 below shows the dependence of the formation energy vs. NS thickness in term of the number of layers. This shows that by increasing the NS thickness the formation energy is lowering, which results in the more stability.

3.2 Thermodynamical stability

To confirm the dynamical stability, phonon dispersion of all the porous NS phases have been calculated using finite displacement method as implemented in the phonopy program [32]. All phonon spectra results are shown in Figure 2, we have found that all the vibrational frequencies of NS series are positive in the first Brillouin zone, demonstrating clearly that studied NS phases are dynamically stable, i.e. they are located at the real minimum of the potential energy surface. We note that for all NS, a remarkable phonon gap is observed in the phonon spectra.

3.3 Mechanical stability

While the phonon calculation is the test of whether a proposed 2D configuration would be dynamically stable, or the structure represents a minimum of the potential energy surface. It is necessary to assess also the effect of lattice distortion on structural stability ensuring the *positive-definiteness* of strain energy following lattice distortion. Thus, we have performed a test for the distortion of the NS's unit cell shape, by calculating the components of the stiffness tensor corresponding to uniaxial deformations along the major axis, i.e. the C_{11} , C_{12} and C_{66} components in the Voigt notation. As suggested in [33,34] the material structure is considered as mechanically stable if they obey the Born–Huang criteria. In our 2D NS case, the three following criteria are met (i) $C_{11} > 0$, (ii) $C_{66} > 0$ and (iii) $C_{11} > |C_{12}|$. The stiffness and compliance tensor of all NS structures are given in Table 1 as component C_{11} , C_{12} and C_{66} (in our tetragonal NS's symmetry the $C_{11} = C_{22}$).



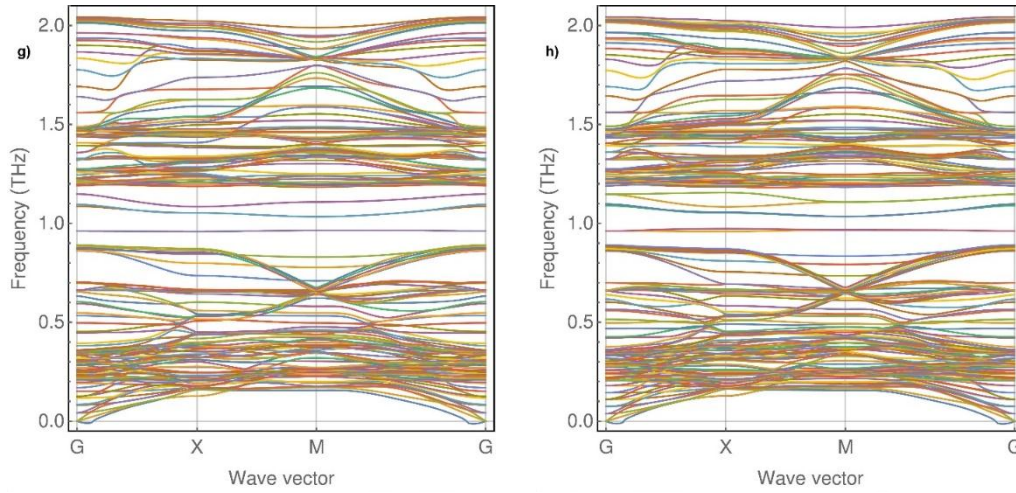


Figure 2. Phonon spectra of the studied NS series: a) SOD-1, b) SOD-2, c) SOD-3, d) SOD-4, e) SOD-5, f) SOD-6, g) SOD-7, h) SOD-8.

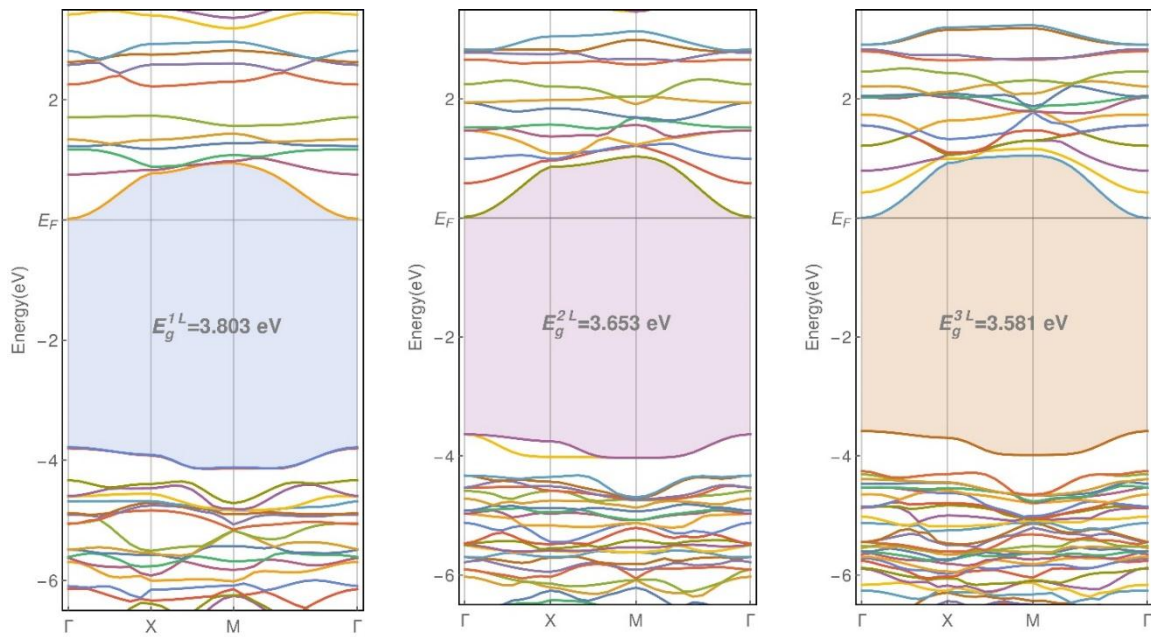


Figure 3. Band structure of some representative NS structure. Fermi energies are set to zero. Gap value and the structures name is in the graphs.

3.4 Electronic band structure

Determining whether the nanoporous NS phases, if synthesized, would possess novel properties, we explore their electronic structures. Figure 3 shows the band structures of some smallest NS structures, i.e. SOD-1, SOD2 and SOD-3. It is noted that their gap fall below the bulk porous SOD phase value (4.26eV) and the ZnO wurtzite phase. Our calculations show that the band gap of the series varies from

3.43eV to 3.89eV among the series. It is also should be noted that within the used scheme, DFTB+ calculations overestimate the band gap, which is 3.44 eV for wurtzite ZnO from low temperature experimental measurements [35]. To benchmark of this value, by DFTB+ we obtained the ZnO wurtzite band gap of 4.16eV and ZnO zinblende band gap is 3.73eV, which can be considered close enough to the above experimental value. Thus, these results show that all the new 2D porous NS are still wide band gap semiconducting, though smaller than wurtzite one, with direct gap at the Gamma point (see Figure 3). On the other hand, the designed NS's result in major differences with bulk phase in electronic band flattening at the valence band (see Figure 3). The reason for this observation, is due to the void open in the cage parent's structure restricting band-forming capacity. Further we also observed the dependence of band gap on the NS thickness measured here in the number of the layers (see Figure 4) as the band-gap energy decreases with the increasing the number of the mono-block layer, i.e. the thickness. This dependence is follow up the rule of quantum confinement. Overall, our result confirms that the energy gap of the porous NS's series, which is an important parameter towards technological applications, is sensitive to NS thickness.

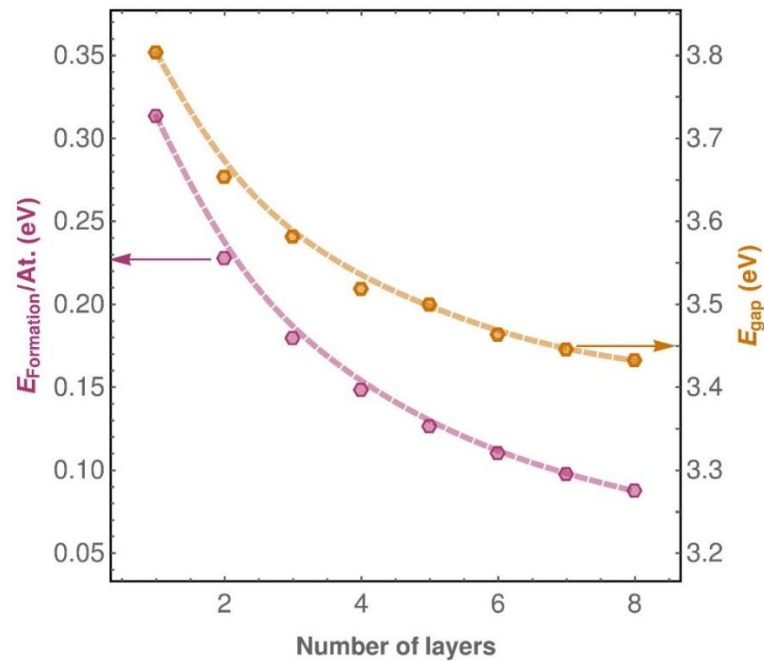


Figure 4. The dependence of the formation energy (left axis) and the band gap (right axis) on the NS thickness (in number of layers).

4. Other remarks

Because the calculated elastic constants of all studied phases satisfy the Born–Huang stability conditions, we conclude that our proposed porous NS structures are mechanically stable. Further to estimate the dependence of the relative strength of these porous NS phases, we have shown in Figure 5 the dependence of the NS series elastic constant on their thickness, in term of the number of mono-block layer. Which shows that all the elastic constants go up almost linearly with the increasing of the NS thickness, see the dashed lines in Figure 5, which show the going trend (see also Table 1).

Table 1. Calculated characteristics of the studied structures.

| Structures | SOD-1 | SOD-2 | SOD-3 | SOD-4 | SOD-5 | SOD-6 | SOD-7 | SOD-8 |
|---|------------------|------------------|------------------|------------------|------------------|------------------|------------------|------------------|
| Coord. number | 3.50 | 3.64 | 3.71 | 3.76 | 3.80 | 3.83 | 3.85 | 3.86 |
| Crystal structure | Tetrag. |
| Symmetry groups | Pmmm IT 47 | P-4m2 IT 115 |
| Unit cell (atoms) | 16 | 22 | 28 | 34 | 40 | 46 | 52 | 58 |
| In-plane Lat. param. Å (a,b) | 5.941 5.958 | 5.868 5.868 | 5.810 5.851 | 5.811 5.811 | 5.780 5.815 | 5.789 5.789 | 5.767 5.796 | 5.778 5.778 |
| Average bond Å | 1.993 ±0.069 | 2.004 ±0.063 | 2.010 ±0.056 | 2.014 ±0.051 | 2.016 ±0.047 | 2.018 ±0.044 | 2.019 ±0.041 | 2.020 ±0.039 |
| Average angle Zn-O-Zn/O-Zn-O | 108.96 112.09 | 109.08 117.74 | 109.23 111.28 | 109.34 111.03 | 109.44 110.85 | 109.50 110.73 | 109.56 110.63 | 109.60 110.57 |
| Formation ener//at. (eV) | 0.313 | 0.227 | 0.179, | 0.148 | 0.126 | 0.110 | 0.097 | 0.087 |
| Band gap eV | 3.803 | 3.653 | 3.581 | 3.518 | 3.499 | 3.463 | 3.445 | 3.432 |
| NS's Connolly surface area Å ² | 141.37 | 181.22 | 225.28 | 265.26 | 303.89 | 344.52 | 385.41 | 425.33 |
| Stiffness tensor C ₁₁ (N/m) | 54.693 | 94.595 | 116.27 | 158.28 | 179.83 | 222.11 | 243.62 | 285.939 |
| C ₁₂ (N/m) | 14.637 | 17.434 | 39.849 | 41.175 | 63.728 | 65.084 | 87.538 | 88.736 |
| C ₆₆ (N/m) | 3.177 | 4.412 | 5.725 | 7.032 | 8.365 | 9.680 | 11.015 | 12.382 |
| Complian.tensor S ₁₁ (N/m) | 0.0197 | 0.011 | 0.010 | 0.0068 | 0.0064 | 0.0049 | 0.0047 | 0.0039 |
| S ₁₂ (N/m) | -0.005 | -0.002 | -0.003 | -0.002 | -0.002 | -0.001 | -0.001 | -0.001 |
| S ₆₆ (N/m) | 0.3147 | 0.2267 | 0.1747 | 0.1422 | 0.1195 | 0.1033 | 0.0908 | 0.0808 |

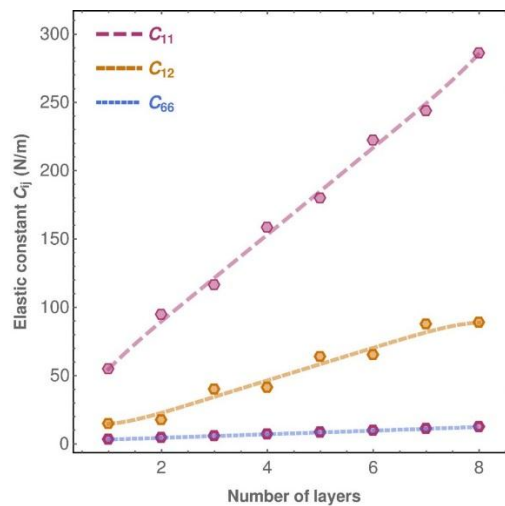


Figure 5. The dependence of the NS's elastic constants (stiffness tensor components) vs thickness.

Naturally, it leads to higher flexibility and compressibility (with the lower constants) of this new series of porous NS phases. Therefore, these new nanoporous phases if synthesized, will be the promising candidates of mechanical meta-materials for replacing the expensive and mechanically fragile atomic or molecular selective materials. Their gap-engineering and large internal surface area of the hollow cage-host also serve as promising solutions for efficient solar-to-chemical energy conversion and photo-electrochemical water splitting alternately to TiO₂ micro/nano patterned structures.

5. Conclusions

To date, the porous few-layer thin NS materials have been increasingly important because not only represent the scaling down in the thickness, but might also bring a possibility of tailoring their novel electronic, optical, and mechanical properties for various electronics and photo-catalytic device applications. We have proposed novel porous NS structures of the few mono-block-layer of ZnO SOD phases. Our analysis on their structural, electronics, mechanical and the thermodynamic properties clearly reveal that, these structures may describe the real porous low-density ultrathin nanosheet materials. The important factors for practical application are their ability for gap-engineering and the linear trend of sheet elastic strength with the thickness. Furthermore, we believe that these nanoporous sheets structures can be the prototype for other II-VI semiconducting materials, such as ZnS, CdSe, and CdTe.

Acknowledgments

This work was supported by Vietnam National Foundation for Science and Technology Development (NAFOSTED) under grant number 103.01-2017.24.

References

- [1] J. Jiang, J. Pi, J. Cai, Review Article: The Advancing of Zinc Oxide Nanoparticles for Biomedical Application, *Bioinorg. Chem. Appl.* Vol. 2018, (2018) 1062562, <https://www.hindawi.com/journals/bca/2018/1062562>.
- [2] M.A. Borysiewicz, ZnO as a Functional Material, a Review *Crystals* Vol. 9, (2019) 505, <https://doi.org/10.3390/cryst9100505>
- [3] W.J. Roth, P. Nachtigall, R.E. Morris, P.S. Wheatley, V.R. Seymour, S.E. Ashbrook, P. Chlubná, L. Grajciar, M. Položij, A. Zukal, J. Čejka, A family of zeolites with controlled pore size prepared using a top-down method, *Nat. Chem.* 5 (2013) 628, <https://doi.org/10.1038/nchem.1662>.
- [4] Y. Tian, Y. Zhang, T. Wang, H.L. Xin, H. Li, O. Gang, Lattice engineering through nanoparticle-DNA frameworks, *Nat. Mater.* 15 (2016) 654-661, <https://doi.org/10.1038/nmat457>.
- [5] H. Xiong, M. Y. Sfeir, O. Gang, Assembly, structure and optical response of three-dimensional dynamically tunable multicomponent superlattices, *Nano Lett.* 10 (2010) 4456–4462, <https://doi.org/10.1021/nl102273c>.
- [6] A. Kołodziejczak-Radzimska and T. Jesionowski, Zinc Oxide-From Synthesis to Application: A Review, *Materials* 7 (2014) 2833-2882, <https://doi.org/10.3390/ma7042833>.
- [7] Y. Yong, Song B., He P., Growth Pattern and Electronic Properties of Cluster-Assembled Material Based on Zn₁₂O₁₂: A Density-Functional Study, *J. Phys. Chem. C* 115 (2011) 6455-6461, <https://doi.org/10.1021/jp200780k>.
- [8] I. Demiroglu, S. Tosoni, F. Illasa, S.T. Bromley, Bandgap engineering through nanoporosity, *Nanoscale* 6 (2014) 1181-1187, <https://doi.org/10.1039/C3NR04028C>.
- [9] Z. Liu, X. Wang, J. Cai, G. Liu, P. Zhou, K. Wang, H. Zhu, From the ZnO Hollow Cage Clusters to ZnO Nanoporous Phases: A First-Principles Bottom-Up Prediction, *J. Phys. Chem. C* 117 (2013) 17633-17643, <https://doi.org/10.1021/jp405084r>.
- [10] S.M. Woodley, R. Catlow, Crystal structure prediction from first principles, *Nat. Mater.* 7 (2008) 937-946, <https://doi.org/10.1038/nmat2321>.

- [11] A.A. Sokol, M.R. Farrow, J. Buckeridge, A.J. Logsdail, C.R.A. Catlow, D.O. Scanlonab, S.M. Woodley, Double bubbles: a new structural motif for enhanced electron-hole separation in solids, *Phys. Chem. Chem. Phys.* 16 (2014) 21098-21105, <https://doi.org/10.1039/C4CP01900H>.
- [12] S.T. Bromley, M.A. Zwijnenburg, *Computational Modeling of Inorganic Nanomaterials* 1st Edition, Series: Series in Materials Science and Engineering. CRC Press, May 2, 2016.
- [13] J. Carrasco, F. Illas and S.T. Bromley, Ultralow-Density Nanocage-Based Metal-Oxide Polymorphs, *Phys. Rev. Lett.*, Vol. 99 (2007) 235502, <https://doi.org/10.1103/PhysRevLett.99.235502>.
- [14] V.N. Tuoc, T.D. Huan, N.V. Minh, N.T. Thao, Density functional theory based tight binding study on theoretical prediction of low-density nanoporous phases ZnO semiconductor materials, *J. of Phys. Conf. Series*, Vol. 726 (2016) 012022, <https://doi.org/10.1088/1742-6596/726/1/012022/meta>.
- [15] R. Rasoulkhani, H. Tahmasbi, S. A. Ghasemi, S. Faraji, S. Rostami, and M. Amsler, Energy landscape of ZnO clusters and low-density polymorphs, *Phys. Rev. B*, Vol. 96 (2017) 064108, <https://doi.org/10.1103/PhysRevB.96.064108>.
- [16] V.N. Tuoc, L.T.H. Lien, T.D. Huan, N.T. Thao, Novel cage-like nanoporous ZnO polymorphs with cubic lattice frameworks, *J. of Mater. Today Commun.*, 24 (2020) 101152, <https://doi.org/10.1016/j.mtcomm.2020.101152>.
- [17] V.N. Tuoc, T.D. Huan, N.T. Thao, L.M. Tuan, Theoretical prediction of low-density hexagonal ZnO hollow structures, *J. of Appl. Phys.* 120 (2016) 142195, <https://doi.org/10.1063/1.4961716>.
- [18] V.N. Tuoc, T.D. Huan, N.T. Thao, Computational predictions of zinc oxide hollow structures, *Physica B*, Vol. 532 (2018) 15-19, <https://doi.org/10.1016/j.physb.2017.03.001>.
- [19] S. M. Woodley and R. Catlow, Crystal structure prediction from first principles, *Nat. Mater.* 7 (2008) 937-946, <https://doi.org/10.1038/nmat2321>.
- [20] A. A. Sokol, M. R. Farrow, J. Buckeridge, A. J. Logsdail, C. R. A. Catlow, D. O. Scanlonab, and S. M. Woodley, Double bubbles: a new structural motif for enhanced electron-hole separation in solids, *Phys. Chem. Chem. Phys.* 16 (2014) 21098-21105, <https://doi.org/10.1039/C4CP01900H>.
- [21] M. Elstner, D. Porezag, G. Jungnickel, J. Elsner, M. Haugk, Th. Frauenheim, S. Suhai, and G. Seifert, Self-consistent-charge density-functional tight-binding method for simulations of complex materials properties, *Phys. Rev. B* 58 (1998) 7260, <https://doi.org/10.1103/PhysRevB.58.7260>.
- [22] C. Kohler, G. Seifert, and T. Frauenheim, Density functional based calculations for Fen ($n \leq 32$), *Chem. Phys.* 309 (2005) 23-31, <https://doi.org/10.1016/j.chemphys.2004.03.034>.
- [23] B. Aradi, B. Hourahine, and Th. Frauenheim, DFTB+, a Sparse Matrix-Based Implementation of the DFTB Method, *J. Phys. Chem. A* 111 (2007) 5678-5684, <https://doi.org/10.1021/jp070186p>.
- [24] DFTB+ method <http://www.dftb-plus.info/> (2020) (accessed 10 August 2020).
- [25] V.N. Tuoc, The self-consistent charge density functional tight binding study on wurtzite nanowire, *Comput. Mater. Sci.* 49 (2010) S161-S169, <https://doi.org/10.1016/j.commat.2009.12.031>.
- [26] N.H. Moreira, G. Dolgonos, B. Aradi, A.L. da Rosa, Th. Frauenheim, Toward an Accurate Density-Functional Tight-Binding Description of Zinc-Containing Compounds, *J. Chem. Theory Comput.* 5 (2009) 605-614, <https://doi.org/10.1021/ct800455a>.
- [27] G. Kresse, J. Furthmüller, Efficiency of ab-initio total energy calculations for metals and semiconductors using a plane-wave basis set, *Comput. Mater. Sci.* 6 (1996) 15-50, [https://doi.org/10.1016/0927-0256\(96\)00008-0](https://doi.org/10.1016/0927-0256(96)00008-0).
- [28] G. Kresse, J.J. Furthmüller, Efficient iterative schemes for ab initio total-energy calculations using a plane-wave basis set, *Phys. Rev. B* 54 (1996) 11169, <https://doi.org/10.1103/PhysRevB.54.11169>.
- [29] J.P. Perdew, K. Burke, and M. Ernzerhof, Generalized Gradient Approximation Made Simple, *Phys. Rev. Lett.* 77 (1996) 3865, <https://doi.org/10.1103/PhysRevLett.77.3865>.
- [30] J.P. Perdew, A. Ruzsinszky, G.I. Csonka, O.A. Vydrov, G.E. Scuseria, L.A. Constantin, X. Zhou, and K. Burke, Restoring the Density-Gradient Expansion for Exchange in Solids and Surfaces, *Phys. Rev. Lett.* 100 (2008) 136406, <https://doi.org/10.1103/PhysRevLett.100.136406>.
- [31] J. Heyd, G.E. Scuseria, and M. M. Ernzerhof, Hybrid functionals based on a screened Coulomb potential *J. Chem. Phys.* 124 (2006) 219906, <https://doi.org/10.1063/1.1564060>.
- [32] A.Togo, F. Oba, F. Tanaka, First-principles calculations of the ferroelastic transition between rutile-type and CaCl₂-type SiO₂ at high pressures, *Phys. Rev. B*, Vol. 78 (2008) 134106, <https://doi.org/10.1103/PhysRevB.78.134106>.
- [33] S. Hastrup, M. Strange, M. Pandey, T. Deilmann, P. S Schmidt, N. F Hinsche, M. N Gjerding, D. Torelli, P. M Larsen, A. C Riis-Jensen, The Computational 2D Materials Database: high-throughput modeling and discovery of atomically thin crystals, *2D Mater.* 6 (2019) 048001, <https://doi.org/10.1088/2053-1583/aacfc1>.
- [34] Mounet, N., Gibertini, M., Schwaller, Two-dimensional materials from high-throughput computational exfoliation of experimentally known compounds, *Nat. Nanotech* 13 (2018) 246, <https://doi.org/10.1038/s41565-017-0035-5>.